Pulsed Electromagnetic Field Interaction With a Transmission Line
An Analytical Traveling-Wave Approach Based on Reciprocity

Stumpf, Martin; Antonini, Giulio; Lager, Ioan E.; Ekman, Jonas

DOI
10.1109/TAP.2025.3546055

Publication date
2025

Document Version
Final published version

Published in
IEEE Transactions on Antennas and Propagation

Pulsed Electromagnetic Field Interaction With a Transmission Line: An Analytical Traveling-Wave Approach Based on Reciprocity

Martin Štumpf, *Senior Member, IEEE*, Giulio Antonini, *Fellow, IEEE*, Ioan E. Lager, *Senior Member, IEEE*, and Jonas Ekman, *Member, IEEE*

***Abstract*— Pulsed electromagnetic (EM) field signal transfer from a general EM source distribution to a transmission line (TL) is analyzed with the aid of Lorentz's reciprocity theorem. In this fashion, the transient voltage induced by the impulsive EM source is expressed through the EM fields as radiated by the TL. These transmitted EM fields are expressed in closed form using an analytical procedure that resembles the Cagniard–De Hoop (CdH) technique. The validity of the proposed reciprocity-based methodology is verified with the aid of an alternative analytical solution describing the EM field signal transfer excited by an impulsive vertical electric dipole (VED). Illustrative numerical examples are presented.**

***Index Terms*— Cagniard–De Hoop (CdH) technique, electromagnetic (EM) field transfer, electromagnetic reciprocity, reciprocity theorem, time-domain (TD) analysis, transmission line (TL), traveling-wave antenna.**

I. Introduction

QUANTIFYING the impact of pulsed electromagnetic (EM) fields on transmission lines (TLs) is a matter of paramount concern for securing the high reliability of both electric power distribution and communication systems (e.g., [1], [2], [3], [4]). To estimate these effects, differential coupling models based on TL equations are traditionally employed [5], [6], [7], [8], [9]. Recently, an integral form of the standard (differential) TL coupling models has been introduced in [10] using the Lorentz reciprocity theorem [11, Sec. 28.2]. This coupling model is represented via a reciprocity relation of the time-convolution type (see [12, Eq. (1)]) through which the equivalent time-domain (TD) Thévenin-voltage responses are expressed via (integration of) the excitation EM fields (see [12, Eq. (2)]). Under certain special circumstances, the integrals are amenable to solution by analytical means (e.g., [12], [13], [14] and [15, Ch. 12 and 13]), which makes it possible to solve relatively complex EM scattering problems in an accurate and computationally effortless manner. To enable a straightforward incorporation of more complex EM sources, a novel TD coupling model is proposed in this article. More specifically, without restricting the analysis to time-harmonic EM plane waves (e.g., [16], [17], [18], [19]), the voltage response of a TL is first related to (the interaction of) the volume source distribution of excitation EM fields and the impulse-excited radiated EM fields [20]. As these fields are not necessarily limited to the far-field region, their TD computation is generally a tough task. This difficulty is in the present work circumvented with the aid of a dedicated inversion technique that bears a similarity with the Cagniard–De Hoop (CdH) technique [21]. Although the applied inversion strategy is capable of yielding remarkably straightforward closed-form expressions for transient wave fields radiated from nonstationary sources, it seems that its applications have been thus far limited to the study of EM radiation from an infinite periodic line array of sequentially pulsed axial dipoles [22] and from a dielectric coated thin-wire segment [23]. Accordingly, the presented TD expressions for the radiated transient EM fields are, in their present compact form, believed to be new.

In addition to describing the pulsed EM transfer from an external EM source to a TL using the TD reciprocity theorem (see [12], [13]), the presented closed-form TD expressions can be readily used to study the TD EM radiation from traveling-wave thin-wire antennas (e.g., [24], [25]). Moreover, as TL models are useful for explaining the operation of leaky wave antennas [26], it is anticipated that the presented (CdH-like) inversion procedure will enable us to deepen our understanding of space-time leaky wave phenomena [27], [28].

The analyzed problem configuration is described in Section II. Subsequently, the actual (receiving) situation is in Section III analyzed via the EM reciprocity theorem. Here, it is shown that the TD voltage induced by an external EM source can be expressed via the EM fields radiated from an electric-current impulse traveling along the TL. It is further demonstrated that such EM fields can be expressed in closed

Received 1 November 2024; revised 7 February 2025; accepted 14 February 2025. Date of publication 4 March 2025; date of current version 4 June 2025. This work was supported in part by Czech Science Foundation under Grant 25-15862S. *(Corresponding author: Martin Štumpf.)*

Martin Štumpf is with the Lerch Laboratory of EM Research, Department of Radio Electronics, FEEC, Brno University of Technology, 616 00 Brno, Czech Republic, and also with the Department of Computer Science, Electrical and Space Engineering, EISLAB, Luleå University of Technology, 971 87 Luleå, Sweden (e-mail: martin.stumpf@centrum.cz).

Giulio Antonini is with the UAq EMC Laboratory, Department of Industrial and Information Engineering and Economics, University of L'Aquila, 671 00 L'Aquila, Italy (e-mail: giulio.antonini@univaq.it).

Ioan E. Lager is with the Terahertz Sensing Group, Faculty of Electrical Engineering, Mathematics and Computer Science, Delft University of Technology, 2628 CD Delft, The Netherlands (e-mail: i.e.lager@tudelft.nl).

Jonas Ekman is with the Department of Computer Science, Electrical and Space Engineering, EISLAB, Luleå University of Technology, 971 87 Luleå, Sweden (e-mail: jonas.ekman@ltu.se).

Digital Object Identifier 10.1109/TAP.2025.3546055

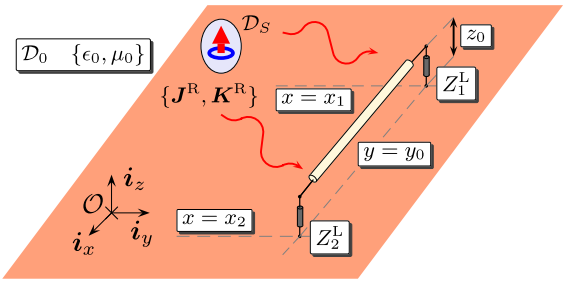

Fig. 1. TL that is irradiated by external EM sources.

form with the aid of an analytical CdH-like inversion procedure, thereby yielding an accurate and efficient EM coupling model. Its analytical details are summarized in Appendix A. To demonstrate the use of the (general) solution methodology, a vertical electric dipole (VED) excited TL is closely analyzed in the ensuing Section IV. Using the corresponding closed-form analytical solution [13], expressions of which are confined to Appendix B, the proposed solution methodology is successfully validated in Section V. Finally, we draw conclusion in Section VII.

II. Problem Description

We shall analyze the TD response of a TL due to externally disturbing EM fields. The corresponding problem configuration is shown in Fig. 1. In it, the spatial position is localized using the Cartesian coordinates $\{x, y, z\}$ with respect to an orthogonal Cartesian reference frame with the origin $\mathcal{O}$ and the standard base vectors $\{\boldsymbol{i}_x, \boldsymbol{i}_y, \boldsymbol{i}_z\}$. The position vector can be then expressed as $\boldsymbol{r} = x\boldsymbol{i}_x + y\boldsymbol{i}_y + z\boldsymbol{i}_z$.

The time coordinate is denoted by t. The Heaviside unit-step function is represented by $\mathrm{H}(t)$ ($\mathrm{H}(t) = 0$ if $t < 0$, $\mathrm{H}(0) = 1/2$ and $\mathrm{H}(t) = 1$ if $t > 0$) and the Dirac-delta distribution is denoted $\delta(t)$. The time convolution is denoted by $*_t$. Then, the time-integration operator can be defined as $\partial_t^{-1} f(t) = f(t) *_t \mathrm{H}(t)$.

The TL is located in a homogeneous, isotropic, and lossless medium above a perfectly electrically conducting (PEC) ground plane. The TL occupies a bounded domain of space that is enclosed by a sufficiently regular surface $\mathcal{S}_0$ [10, Fig. 1]. The ports of the TL at $x = x_{1,2}$ are bounded by internal surfaces $\mathcal{S}_{1,2}$, respectively. Their outer normal unit vector is denoted by $\boldsymbol{\nu}(\boldsymbol{r})$. The ambient medium is described by its electric permittivity, ϵ_0, and magnetic permeability, μ_0. The corresponding EM wave speed and impedance are $c_0 = (\epsilon_0\mu_0)^{-1/2} > 0$ and $\zeta_0 = c_0\mu_0$, respectively. The horizontal conductor of the TL extends over $\mathcal{L} = \{x_1 \leq x \leq x_2, y = y_0, z = z_0\}$, where $z_0 > 0$ is its (relatively small) height above the ground plane. Consequently, the length of the TL is $\ell = x_2 - x_1 > 0$.

The TL is irradiated by external EM fields that are generated by EM sources distributed in a bounded domain $\mathcal{D}_S$. These sources are represented by the electric-current volume density, $\boldsymbol{J}^{\mathrm{R}}(\boldsymbol{r}, t)$, or/and the magnetic-current volume density, $\boldsymbol{K}^{\mathrm{R}}(\boldsymbol{r}, t)$. The voltage and current quantities at the end points at $x = x_{1,2}$ are represented $V_{1,2}(t)$ and $I_{1,2}(t)$, respectively. Within the reciprocity-based analysis that follows, these quantities will be further supplemented with a superscript to denote the pertaining EM-field state. The EM sources are activated at $t = 0$. Prior to this instant, the EM fields are identically zero throughout the problem configuration.

III. Problem Solution

The causality and the time invariance of the EM waves are accounted for through the use of the unilateral Laplace transform

$$\hat{f}(s) = \int_{t=0}^{\infty} \exp(-st) f(t) \mathrm{d}t \tag{1}$$

where the Laplace-transform parameter s is assumed to be real-valued and positive. Consequently, Lerch's uniqueness theorem [29, Appendix] ensures the existence of a one-to-one mapping between the (causal) original, $f(t)$, and its Laplace-transform counterpart, $\hat{f}(s)$. Owing to the zero initial condition, (1) entails the property $\partial_t \to s$.

A. Reciprocity Analysis

The proposed solution methodology is formulated using the s-domain EM reciprocity theorem of the time-convolution type [11, Sec. 28.4] and follows essentially the lines of reasoning presented in [20] (see also [15, Ch. 11] and [29, Sec. 5.1.2]). Accordingly, the actual (receiving) situation (see Fig. 1) (denoted by superscript $^{\mathrm{R}}$) is related to the transmitting state (denoted by superscript $^{\mathrm{T}}$) that corresponds to the operational situation when the TL is at its port excited by a lumped electric-current source (see Figs. 2 and 3).

First, the reciprocity theorem is applied to the domain that is externally bounded by $\mathcal{S}_0$ and internally by $\mathcal{S}_{1,2}$ enclosing the ports at $x = x_{1,2}$. Over $\mathcal{S}_{1,2}$, the EM fields can be expressed in terms of Kirchhoff-circuit quantities (see [20, Eq. (64)] and [29, Sec. 1.5.2])

$$\begin{aligned}\int_{\boldsymbol{r}\in\mathcal{S}_0} \left(\hat{\boldsymbol{E}}^{\mathrm{R}} \times \hat{\boldsymbol{H}}^{\mathrm{T}} - \hat{\boldsymbol{E}}^{\mathrm{T}} \times \hat{\boldsymbol{H}}^{\mathrm{R}}\right) \cdot \boldsymbol{\nu}\, \mathrm{d}A \\ = \hat{V}_1^{\mathrm{R}}\hat{I}_1^{\mathrm{T}} - \hat{V}_1^{\mathrm{T}}\hat{I}_1^{\mathrm{R}} - \hat{V}_2^{\mathrm{R}}\hat{I}_2^{\mathrm{T}} + \hat{V}_2^{\mathrm{T}}\hat{I}_2^{\mathrm{R}}\end{aligned} \tag{2}$$

where we adhered to the orientation of electric currents that is conventional in the TL theory. In the second step, the reciprocity theorem is applied to the unbounded domain *exterior* to $\mathcal{S}_0$. Owing to the explicit-type boundary conditions on the PEC ground and the property of causality of the EM fields [29, Sec. 1.4.3], the reciprocity theorem yields

$$\begin{aligned}\int_{\boldsymbol{r}\in\mathcal{S}_0} \left(\hat{\boldsymbol{E}}^{\mathrm{R}} \times \hat{\boldsymbol{H}}^{\mathrm{T}} - \hat{\boldsymbol{E}}^{\mathrm{T}} \times \hat{\boldsymbol{H}}^{\mathrm{R}}\right) \cdot \boldsymbol{\nu}\, \mathrm{d}A \\ = \int_{\boldsymbol{r}\in\mathcal{D}_S} \left(\hat{\boldsymbol{K}}^{\mathrm{R}} \cdot \hat{\boldsymbol{H}}^{\mathrm{T}} - \hat{\boldsymbol{J}}^{\mathrm{R}} \cdot \hat{\boldsymbol{E}}^{\mathrm{T}}\right) \mathrm{d}V.\end{aligned} \tag{3}$$

Combining next (2) with (3) we end up with

$$\begin{aligned}\hat{V}_1^{\mathrm{R}}\hat{I}_1^{\mathrm{T}} - \hat{V}_1^{\mathrm{T}}\hat{I}_1^{\mathrm{R}} - \hat{V}_2^{\mathrm{R}}\hat{I}_2^{\mathrm{T}} + \hat{V}_2^{\mathrm{T}}\hat{I}_2^{\mathrm{R}} \\ = \int_{\boldsymbol{r}\in\mathcal{D}_S} \left(\hat{\boldsymbol{K}}^{\mathrm{R}} \cdot \hat{\boldsymbol{H}}^{\mathrm{T}} - \hat{\boldsymbol{J}}^{\mathrm{R}} \cdot \hat{\boldsymbol{E}}^{\mathrm{T}}\right) \mathrm{d}V\end{aligned} \tag{4}$$

which relates the (desired) induced voltages/currents at the ports of the TL, $\{\hat{V}_{1,2}^{\mathrm{R}}, \hat{I}_{1,2}^{\mathrm{R}}\}$, with the (known) external sources, $\{\hat{\boldsymbol{J}}^{\mathrm{R}}, \hat{\boldsymbol{K}}^{\mathrm{R}}\}$, through (yet unspecified) testing-state quantities, $\{\hat{\boldsymbol{E}}^{\mathrm{T}}, \hat{\boldsymbol{H}}^{\mathrm{T}}\}$. Two particular testing states are further discussed in detail.

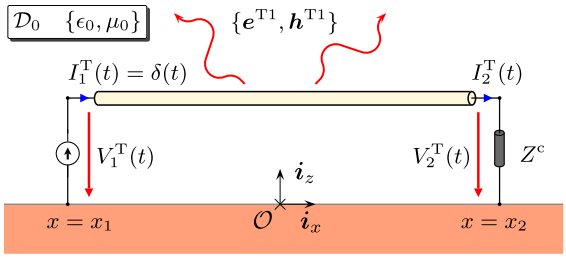

Fig. 2. Transmitting state in which the port at $x = x_1$ is excited and the port at $x = x_2$ is matched.

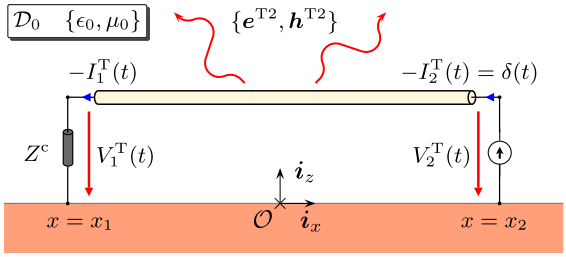

Fig. 3. Transmitting state in which the port at $x = x_2$ is excited and the port at $x = x_1$ is matched.

1) Near-End Thévenin's Voltage: Assuming that the TL is at $x = x_2$ matched in both (T) and (R) states, that is, $Z_2^{\mathrm{L}} = Z_{\mathrm{c}}$, where Z_{c} denotes the characteristic impedance, the reciprocity relation (4) yields the open-circuit Thévenin's voltage induced at $x = x_1$ (i.e., $Z_1^{\mathrm{L}} \to \infty$)

$$\hat{V}_1^{\mathrm{G}}(s) = \int_{\boldsymbol{r} \in \mathcal{D}_S} \left(\hat{\boldsymbol{K}}^{\mathrm{R}} \cdot \hat{\boldsymbol{h}}^{\mathrm{T}1} - \hat{\boldsymbol{J}}^{\mathrm{R}} \cdot \hat{\boldsymbol{e}}^{\mathrm{T}1} \right) \mathrm{d}V \tag{5}$$

where we have introduced the impulse-excited transmitted fields according to

$$\{\hat{\boldsymbol{e}}^{\mathrm{T}1}, \hat{\boldsymbol{h}}^{\mathrm{T}1}\} = \{\hat{\boldsymbol{E}}^{\mathrm{T}}, \hat{\boldsymbol{H}}^{\mathrm{T}}\}|_{\hat{I}_1^{\mathrm{T}}=1}. \tag{6}$$

To evaluate the EM fields as radiated from the *horizontal* conductor of a TL that is at $x = x_1$ excited by the impulsive electric-current source and matched at $x = x_2$ (see Fig. 2) we may adopt the methodology that resembles the CdH technique [23] (see Appendix A). The corresponding space-time electric-current distribution traveling in the *positive* x-direction is given by

$$I^{\mathrm{T}}(x, t) = \delta[t - (x - x_1)/c_0]. \tag{7}$$

Consequently, $I^{\mathrm{T}}(x_1, t) = I_1^{\mathrm{T}}(t) = \delta(t)$ and $I^{\mathrm{T}}(x_2, t) = I_2^{\mathrm{T}}(t) = \delta(t - \ell/c_0)$. Finally, the EM fields radiated from the vertical sections along $\{x = x_{1,2}, y = y_0, 0 \le z \le z_0\}$ can be evaluated using the well-known expressions pertaining to the EM radiation from a short, thin-wire segment carrying a uniform electric current [11, Sec. 26.9]. The effect of the PEC ground plane is incorporated through the method of images [11, Sec. 23.2]. This approach is pursued in Section III-B2.

2) Far-End Thévenin's Voltage: Assuming that the TL is at $x = x_1$ matched in both (T) and (R) states, that is, $Z_1^{\mathrm{L}} = Z_{\mathrm{c}}$, where Z_{c} denotes the characteristic impedance, the reciprocity relation (4) yields the open-circuit Thévenin's voltage induced at $x = x_2$ (i.e., $Z_2^{\mathrm{L}} \to \infty$)

$$\hat{V}_2^{\mathrm{G}}(s) = -\int_{\boldsymbol{r} \in \mathcal{D}_S} \left(\hat{\boldsymbol{K}}^{\mathrm{R}} \cdot \hat{\boldsymbol{h}}^{\mathrm{T}2} - \hat{\boldsymbol{J}}^{\mathrm{R}} \cdot \hat{\boldsymbol{e}}^{\mathrm{T}2} \right) \mathrm{d}V \tag{8}$$

where we have introduced the impulse-excited transmitted fields according to

$$\{\hat{\boldsymbol{e}}^{\mathrm{T}2}, \hat{\boldsymbol{h}}^{\mathrm{T}2}\} = \{\hat{\boldsymbol{E}}^{\mathrm{T}}, \hat{\boldsymbol{H}}^{\mathrm{T}}\}|_{\hat{I}_2^{\mathrm{T}}=1}. \tag{9}$$

To evaluate the EM fields as radiated from the *horizontal* conductor of a TL that is at $x = x_2$ excited by the impulsive electric-current source and matched at $x = x_1$ (see Fig. 3) we may again apply the methodology presented in Appendix A. The corresponding space-time electric-current distribution traveling in the *negative* x-direction is given by

$$I^{\mathrm{T}}(x, t) = -\delta[t - (x_2 - x)/c_0]. \tag{10}$$

Consequently, $I^{\mathrm{T}}(x_2, t) = I_2^{\mathrm{T}}(t) = -\delta(t)$ and $I^{\mathrm{T}}(x_1, t) = I_1^{\mathrm{T}}(t) = -\delta(t - \ell/c_0)$. The EM-field radiation from the vertical sections is in Section III-B2 evaluated using the approximation pertaining to a short, thin-wire segment carrying a uniform electric current [11, Sec. 26.9] and the method of images [11, Sec. 23.2].

B. EM Radiation From the TL

In this section, we shall evaluate the EM field radiation from the TL in its (T) states (see Figs. 2 and 3). In this analysis, we shall distinguish between the EM fields radiated from the horizontal (denoted by $^{\mathrm{h}}$) and vertical (denoted by $^{\mathrm{v}}$) sections of the TL. The total EM fields then follow as their superposition, i.e.,

$$\left\{e_{x,y,z}^{\mathrm{T}}, h_{x,y,z}^{\mathrm{T}}\right\} = \left\{e_{x,y,z}^{\mathrm{T;h}} + e_{x,y,z}^{\mathrm{T;v}}, h_{x,y,z}^{\mathrm{T;h}} + h_{x,y,z}^{\mathrm{T;v}}\right\} \tag{11}$$

respectively. The calculation of the radiated EM fields will be accomplished through the standard source-type representations [11, Sec. 26.3].

1) Horizontal Conductor: The nonvanishing EM-field components radiated from the horizontal conductor of the TL can be expressed in the following way.

$$\hat{e}_x^{\mathrm{T;h}} = -s\mu_0 \hat{A}_x + \partial_x^2 \hat{A}_x / s\epsilon_0 \tag{12}$$

$$\hat{e}_y^{\mathrm{T;h}} = \partial_y \partial_x \hat{A}_x / s\epsilon_0 \tag{13}$$

$$\hat{e}_z^{\mathrm{T;h}} = \partial_z \partial_x \hat{A}_x / s\epsilon_0 \tag{14}$$

and

$$\hat{h}_y^{\mathrm{T;h}} = \partial_z \hat{A}_x \tag{15}$$

$$\hat{h}_z^{\mathrm{T;h}} = -\partial_y \hat{A}_x \tag{16}$$

where the s-domain potential function is given by 1-D convolution integrals

$$\hat{A}_x(\boldsymbol{r}, s) = \int_{x'=x_1}^{x_2} \big[\hat{G}(x - x', y - y_0, z - z_0) - \hat{G}(x - x', y - y_0, z + z_0)\big] \hat{I}^{\mathrm{T}}(x', s) \mathrm{d}x' \tag{17}$$

with $\hat{G}(x, y, z) = \exp(-sR/c_0)/4\pi R$, $R = (x^2 + y^2 + z^2)^{1/2}$, and $\hat{I}^{\mathrm{T}}(x, s)$ represents the s-domain counterpart of (7) or (10).

Finally, the use of (17) in (12)–(16) leads to s-domain wave constituents that can be transformed back to TD via the methodology presented in Appendix A. A detailed analysis is provided in Section IV for a VED source represented by $\boldsymbol{J}^{\mathrm{R}} = J_z^{\mathrm{R}} \boldsymbol{i}_z$ and $\boldsymbol{K}^{\mathrm{R}} = \boldsymbol{0}$.

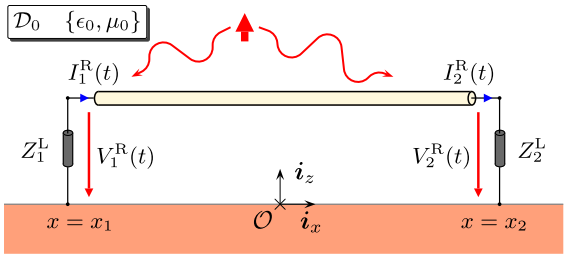

Fig. 4. TL excited by a VED.

2) Vertical Conductor: The non-vanishing EM-field components radiated from the vertical sections of the TL can be expressed via

$$\hat{e}_x^{\mathrm{T;v}} = \partial_x \partial_z \hat{A}_z / s\epsilon_0 \tag{18}$$
$$\hat{e}_y^{\mathrm{T;v}} = \partial_y \partial_z \hat{A}_z / s\epsilon_0 \tag{19}$$
$$\hat{e}_z^{\mathrm{T;v}} = -s\mu_0 \hat{A}_z + \partial_z^2 \hat{A}_z / s\epsilon_0 \tag{20}$$

and

$$\hat{h}_x^{\mathrm{T;h}} = \partial_y \hat{A}_z \tag{21}$$
$$\hat{h}_y^{\mathrm{T;h}} = -\partial_x \hat{A}_z \tag{22}$$

where the potential function represents the radiation from two short thin-wire segments carrying a uniform current distribution, i.e.,

$$\hat{A}_z(\boldsymbol{r}, s) \simeq 2z_0 \hat{I}_1^{\mathrm{T}}(s) \hat{G}(x - x_1, y - y_0, z) - 2z_0 \hat{I}_2^{\mathrm{T}}(s) \hat{G}(x - x_2, y - y_0, z) \tag{23}$$

where the factor 2 accounts for the presence of the PEC ground plane and $\simeq$ indicates that we have approximated the integral $\int_{\zeta=-z_0}^{z_0} \hat{G}(x, y, z - \zeta) \mathrm{d}\zeta$ by $2z_0 \hat{G}(x, y, z)$. Recall that $\hat{I}_1^{\mathrm{T}}(s) = 1$ with $\hat{I}_2^{\mathrm{T}}(s) = \exp(-s\ell/c_0)$ for the transmitting state shown in Fig. 2, while $\hat{I}_1^{\mathrm{T}}(s) = -\exp(-s\ell/c_0)$ with $\hat{I}_2^{\mathrm{T}}(s) = -1$ for the one shown in Fig. 3. Finally, the use of (23) in (18)–(22) leads to s-domain expressions that can be readily transformed back to TD. More details are provided in the following Section IV for a VED source excitation.

IV. VED-Excited TL

The VED-excited TD response of a TL (see Fig. 4) has been described analytically in terms of elementary TD functions in [13] (see [15, Ch. 13] for details) using the CdH technique [21] (see Appendix B). The (reference) CdH solution has been thoroughly validated in [12] and [13] with the aid of finite-difference implementations of the scattered-voltage coupling model [6]. In this section, we shall provide an alternative closed-form solution to this problem that relies on the (general) reciprocity-based solution introduced in Section III.

The action of a VED is described through a localized electric-current volume density, viz

$$\hat{\boldsymbol{J}}^{\mathrm{R}}(\boldsymbol{r}, s) = \hat{i}^{\mathrm{R}}(s) \ell^{\mathrm{R}} \delta(\boldsymbol{r} - \boldsymbol{r}_S) \boldsymbol{i}_z \tag{24}$$

and $\hat{\boldsymbol{K}}^{\mathrm{R}} = \boldsymbol{0}$, where $\hat{i}^{\mathrm{R}}(s)$ denotes the s-domain counterpart of the exciting pulse shape, $\ell^{\mathrm{R}} > 0$ is the length of the dipole and $\boldsymbol{r}_S = x_S \boldsymbol{i}_x + y_S \boldsymbol{i}_y + z_S \boldsymbol{i}_z$ is its position.

Substitution of (24) in (5) and (8), using the sifting property of the Dirac-delta distribution and transforming the thus obtained s-domain expressions into TD, we end up with

$$V_1^{\mathrm{G}}(t) = -\ell^{\mathrm{R}} i^{\mathrm{R}}(t) *_t e_z^{\mathrm{T1}}(\boldsymbol{r}_S, t) \tag{25}$$
$$V_2^{\mathrm{G}}(t) = \ell^{\mathrm{R}} i^{\mathrm{R}}(t) *_t e_z^{\mathrm{T2}}(\boldsymbol{r}_S, t). \tag{26}$$

Recall that e_z^{T1} and e_z^{T2} correspond to the transmitting states shown in Figs. 2 and 3, respectively, and that these radiated EM fields are in general composed of contributions from the horizontal and vertical sections of a TL [see (11)], that is, $e_z^{\mathrm{T1}} = e_z^{\mathrm{T1;h}} + e_z^{\mathrm{T1;v}}$ and $e_z^{\mathrm{T2}} = e_z^{\mathrm{T2;h}} + e_z^{\mathrm{T2;v}}$.

A. VED-Excited TD Near-End Thévenin's Voltage

To evaluate $V_1^{\mathrm{G}}(t)$ according to (25), we shall express the z-component of the electric-field strength as radiated in the corresponding transmitting state (see Fig. 2). To that end, we first pursue the methodology specified in Section III-B1 that yields the contribution from the horizontal conductor, i.e.,

$$V_1^{\mathrm{G;h}}(t) = -\ell^{\mathrm{R}} i^{\mathrm{R}}(t) *_t e_z^{\mathrm{T1;h}}(\boldsymbol{r}_S, t) \tag{27}$$

where

$$\begin{aligned} & i^{\mathrm{R}}(t) *_t e_z^{\mathrm{T1;h}}(\boldsymbol{r}, t) \\ &= \mu_0 \partial_t i^{\mathrm{R}}(t) *_t \left\{ \frac{(z - z_0)[x - x_+(t)]}{R_+^2(t)} \Gamma_+(\boldsymbol{r}, t) - \frac{(z + z_0)[x - x_+^*(t)]}{R_+^{*2}(t)} \Gamma_+^*(\boldsymbol{r}, t) \right\} \\ &\quad + 3\zeta_0 i^{\mathrm{R}}(t) *_t \left\{ \frac{(z - z_0)[x - x_+(t)]}{R_+^2(t)} \frac{\Gamma_+(\boldsymbol{r}, t)}{R_+(t)} - \frac{(z + z_0)[x - x_+^*(t)]}{R_+^{*2}(t)} \frac{\Gamma_+^*(\boldsymbol{r}, t)}{R_+^*(t)} \right\} \\ &\quad + 3\epsilon_0^{-1} \partial_t^{-1} i^{\mathrm{R}}(t) *_t \left\{ \frac{(z - z_0)[x - x_+(t)]}{R_+^2(t)} \frac{\Gamma_+(\boldsymbol{r}, t)}{R_+^2(t)} - \frac{(z + z_0)[x - x_+^*(t)]}{R_+^{*2}(t)} \frac{\Gamma_+^*(\boldsymbol{r}, t)}{R_+^{*2}(t)} \right\}. \end{aligned} \tag{28}$$

The space-time quantities that occur on the right-hand side of (28) have been specified in Appendix A-A. Next, the contribution from the vertical sections of the TL can be found through the approach described in Section III-B2. Indeed, this way readily leads to

$$V_1^{\mathrm{G;v}}(t) = -\ell^{\mathrm{R}} i^{\mathrm{R}}(t) *_t e_z^{\mathrm{T1;v}}(\boldsymbol{r}_S, t) \tag{29}$$

where

$$\begin{aligned} & i^{\mathrm{R}}(t) *_t e_z^{\mathrm{T1;v}}(\boldsymbol{r}, t) \\ &= -\frac{\mu_0 z_0}{2\pi R_1} \left(1 - \frac{z^2}{R_1^2}\right) \partial_t i^{\mathrm{R}}\left(t - \frac{R_1}{c_0}\right) \\ &\quad + \frac{\mu_0 z_0}{2\pi R_2} \left(1 - \frac{z^2}{R_2^2}\right) \partial_t i^{\mathrm{R}}\left(t - \frac{\ell}{c_0} - \frac{R_2}{c_0}\right) \\ &\quad - \frac{\zeta_0 z_0}{2\pi R_1^2} \left(1 - 3\frac{z^2}{R_1^2}\right) i^{\mathrm{R}}\left(t - \frac{R_1}{c_0}\right) \end{aligned}$$

$$+\frac{\zeta_0 z_0}{2\pi R_2^2}\left(1-3\frac{z^2}{R_2^2}\right)i^{\mathrm{R}}\left(t-\frac{\ell}{c_0}-\frac{R_2}{c_0}\right)$$
$$-\frac{z_0}{2\pi\epsilon_0 R_1^3}\left(1-3\frac{z^2}{R_1^2}\right)\partial_t^{-1}i^{\mathrm{R}}\left(t-\frac{R_1}{c_0}\right)$$
$$+\frac{z_0}{2\pi\epsilon_0 R_2^3}\left(1-3\frac{z^2}{R_2^2}\right)\partial_t^{-1}i^{\mathrm{R}}\left(t-\frac{\ell}{c_0}-\frac{R_2}{c_0}\right). \quad (30)$$

In (30), we used $R_{1,2}=[(x-x_{1,2})^2+(y-y_0)^2+z^2]^{1/2}>0$, respectively. The sum of (27) and (29), $V_1^{\mathrm{G;h}}+V_1^{\mathrm{G;v}}$, yields the VED-excited TD near-end voltage response V_1^{G}. The evaluation of the TD expressions is straightforward and does not present any difficulties.

B. VED-Excited TD Far-End Thévenin's Voltage

In this section, we shall employ the TD reciprocity relation (25) to provide closed-form expressions for $V_2^{\mathrm{G}}(t)$. Via the methodology presented in Section III-B1, the z-component of the electric-field strength as radiated from the horizontal conductor in the transmitting shown in Fig. 3 can be found. Along these lines, we arrive at

$$V_2^{\mathrm{G;h}}(t)=\ell^{\mathrm{R}}\, i^{\mathrm{R}}(t)*_t e_z^{\mathrm{T2;h}}(\boldsymbol{r}_S,t) \quad (31)$$

where [see (28)]

$$\begin{aligned}
&i^{\mathrm{R}}(t)*_t e_z^{\mathrm{T2;h}}(\boldsymbol{r},t)\\
&=\mu_0\partial_t i^{\mathrm{R}}(t)*_t\left\{\frac{(z-z_0)[x-x_-(t)]}{R_-^2(t)}\Gamma_-(\boldsymbol{r},t)\right.\\
&\qquad\left.-\frac{(z+z_0)[x-x_-^*(t)]}{R_-^{*2}(t)}\Gamma_-^*(\boldsymbol{r},t)\right\}\\
&\quad+3\zeta_0 i^{\mathrm{R}}(t)*_t\left\{\frac{(z-z_0)[x-x_-(t)]}{R_-^2(t)}\frac{\Gamma_-(\boldsymbol{r},t)}{R_-(t)}\right.\\
&\qquad\left.-\frac{(z+z_0)[x-x_-^*(t)]}{R_-^{*2}(t)}\frac{\Gamma_-^*(\boldsymbol{r},t)}{R_-^*(t)}\right\}\\
&\quad+3\epsilon_0^{-1}\partial_t^{-1}i^{\mathrm{R}}(t)*_t\left\{\frac{(z-z_0)[x-x_-(t)]}{R_-^2(t)}\frac{\Gamma_-(\boldsymbol{r},t)}{R_-^2(t)}\right.\\
&\qquad\left.-\frac{(z+z_0)[x-x_-^*(t)]}{R_-^{*2}(t)}\frac{\Gamma_-^*(\boldsymbol{r},t)}{R_-^{*2}(t)}\right\}.
\end{aligned} \quad (32)$$

The space-time quantities that occur on the left-hand side of (32) have been specified in Appendix A-B. Furthermore, pursuing the approach described in Section III-B2, the contribution from the vertical sections of the TL is given by

$$V_2^{\mathrm{G;v}}(t)=\ell^{\mathrm{R}}\, i^{\mathrm{R}}(t)*_t e_z^{\mathrm{T2;v}}(\boldsymbol{r}_S,t) \quad (33)$$

where [see (30)]

$$\begin{aligned}
&i^{\mathrm{R}}(t)*_t e_z^{\mathrm{T2;v}}(\boldsymbol{r},t)\\
&=\frac{\mu_0 z_0}{2\pi R_2}\left(1-\frac{z^2}{R_2^2}\right)\partial_t i^{\mathrm{R}}\left(t-\frac{R_2}{c_0}\right)\\
&\quad-\frac{\mu_0 z_0}{2\pi R_1}\left(1-\frac{z^2}{R_1^2}\right)\partial_t i^{\mathrm{R}}\left(t-\frac{\ell}{c_0}-\frac{R_1}{c_0}\right)\\
&\quad+\frac{\zeta_0 z_0}{2\pi R_2^2}\left(1-3\frac{z^2}{R_2^2}\right)i^{\mathrm{R}}\left(t-\frac{R_2}{c_0}\right)
\end{aligned}$$

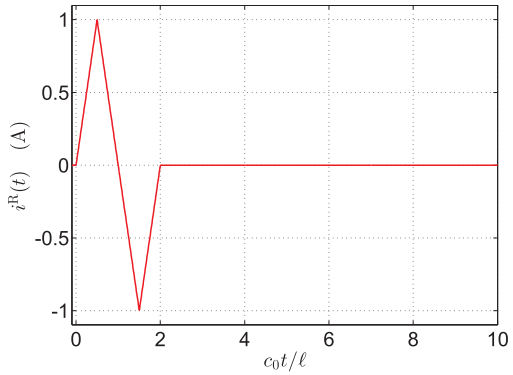

Fig. 5. Excitation electric-current pulse shape.

$$\begin{aligned}
&-\frac{\zeta_0 z_0}{2\pi R_1^2}\left(1-3\frac{z^2}{R_1^2}\right)i^{\mathrm{R}}\left(t-\frac{\ell}{c_0}-\frac{R_1}{c_0}\right)\\
&+\frac{z_0}{2\pi\epsilon_0 R_2^3}\left(1-3\frac{z^2}{R_2^2}\right)\partial_t^{-1}i^{\mathrm{R}}\left(t-\frac{R_2}{c_0}\right)\\
&-\frac{z_0}{2\pi\epsilon_0 R_1^3}\left(1-3\frac{z^2}{R_1^2}\right)\partial_t^{-1}i^{\mathrm{R}}\left(t-\frac{\ell}{c_0}-\frac{R_1}{c_0}\right).
\end{aligned} \quad (34)$$

Finally, the sum of (31) and (33) can be used to calculate the VED-excited TD far-end voltage response V_2^{G}.

V. Numerical Examples

In this section, the closed-form expressions presented in Section IV will be evaluated and validated with the aid of the exact TD solution based on the CdH technique [13] (see Appendix B). To that end, we consider a TL that is located along $\mathcal{L}=\{x_1=-3\ell/4\le x\le x_2=\ell/4, y=y_0=-\ell/10, z=z_0=\ell/50\}$, where we take $\ell=0.10$ m. The TL is excited by a VED source of length $\ell^{\mathrm{R}}=\ell/100$ that is located above the origin at $\boldsymbol{r}_S=z_S\boldsymbol{i}_z$ with $z_S=\ell/8$, without loss of generality due to the (space-time) shift-invariance of the configuration. The dipole is activated at $t=0$ by an electric-current pulse that has the shape of a bipolar triangle

$$\begin{aligned}
&i^{\mathrm{R}}(t)\\
&=(2i_{\mathrm{m}}/t_{\mathrm{w}})\big[t\,\mathrm{H}(t)-2\big(t-t_{\mathrm{w}}/2\big)\mathrm{H}\big(t-t_{\mathrm{w}}/2\big)+2\big(t-3t_{\mathrm{w}}/2\big)\\
&\qquad\times\mathrm{H}\big(t-3t_{\mathrm{w}}/2\big)-(t-2t_{\mathrm{w}})\,\mathrm{H}(t-2t_{\mathrm{w}})\big]
\end{aligned} \quad (35)$$

where we take the unit amplitude, $i_{\mathrm{m}}=1.0$ A and its time width is defined by $c_0t_{\mathrm{w}}=\ell$ (see Fig. 5). The time window of observation is chosen to be $\{0\le c_0t\le 10\,\ell\}$.

Fig. 6 shows the resulting TD Thévenin voltages as computed using the expressions from Section IV (= Reciprocity model) and using the CdH referential solution (see Appendix B). Overall, the results correlate very well. Minor discrepancies at the peaks of the voltage response [see Fig. 6(b)] can be attributed to the approximation involved in the expression for the potential function (23). In the CdH-based solution (= CdH reference), this integration is carried out analytically.

VI. Extensions of the Coupling Model

The pulsed EM source interaction with a TL has been described under simplifying assumptions. In this section,

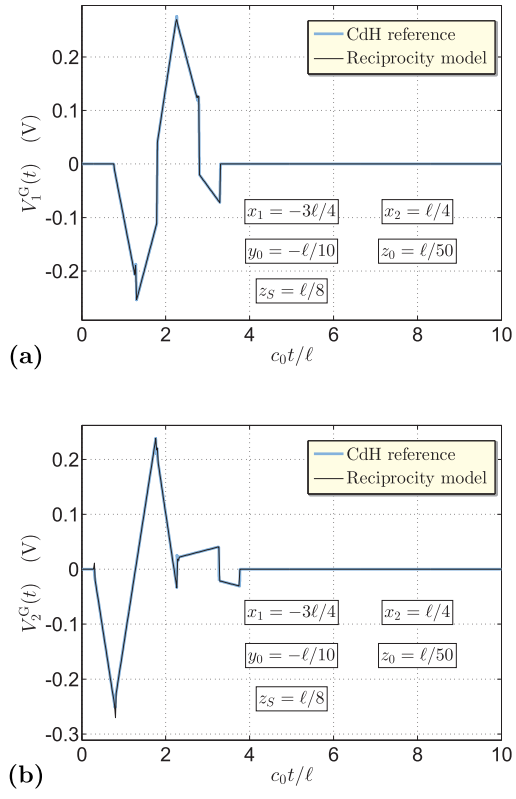

Fig. 6. Thévenin's voltage transient responses. At (a) near-end $x = x_1$ and (b) far-end $x = x_2$.

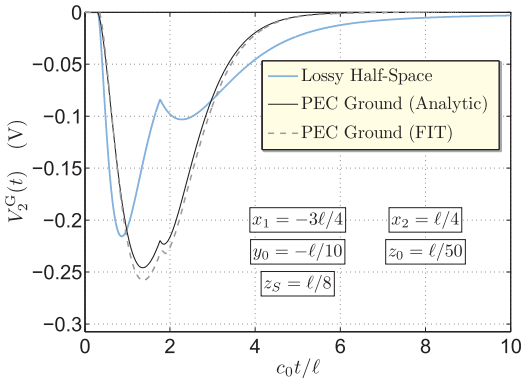

Fig. 7. Thévenin's voltage transient responses at the far-end $x = x_2$ above PEC ground and lossy half-space with $\sigma = 4.0\,\mathrm{S/m}$ and $\epsilon_r = 81$.

we shall describe how the TD model can be applied to more general problem configurations.

1) First, the TD closed-form expressions presented in (see Section IV) apply to a VED source. However, the reciprocity model accounts for the arbitrary space-time distribution of external EM sources. For a horizontal electric dipole source, for instance, one can use [see (24)]

$$\hat{\boldsymbol{J}}^{\mathrm{R}}(\boldsymbol{r}, s) = \hat{i}^{\mathrm{R}}(s)\ell^{\mathrm{R}}\delta(\boldsymbol{r} - \boldsymbol{r}_S)\boldsymbol{i}_r \tag{36}$$

where $\boldsymbol{i}_r = \boldsymbol{i}_x \cos(\phi) + \boldsymbol{i}_y \sin(\phi)$ is a unit vector in the radial direction and ϕ denotes the azimuthal angle of the polar coordinate system. Consequently, the voltage responses are evaluated according to (5) and (8) via the radial components of the impulse-excited transmitted fields. This can be done again using the expressions presented in Section III-B and the transform methodology described in Appendix A. Furthermore, the results of Section V are limited to the bipolar triangle pulse shape of a VED, but any other causal EM pulse can be readily incorporated. Indeed, the power-exponential pulse [30], for example, can serve the purpose [see (35)]

$$i^{\mathrm{R}}(t) = i_{\mathrm{m}}(t/t_{\mathrm{r}})^n \exp[-n(t/t_{\mathrm{r}} - 1)]\mathrm{H}(t) \tag{37}$$

where i_{m} denotes the amplitude, n denotes the rising power, and the pulse time width, t_{w}, follows from the pulse rise time, t_{r}, via $t_{\mathrm{w}} = t_{\mathrm{r}}\, n^{-n-1}\Gamma(n+1)\exp(n)$.

2) The presented TD closed-form expressions are limited to a PEC ground plane. An efficient way to incorporate the effect of finite ground conductivity and permittivity is based on the so-called Cooray–Rubinstein approximation [31], [32]. This strategy has been pursued in [12], where the corresponding voltage corrections (with respect to the ideal PEC case) have been derived analytically using the CdH technique (see [12, Eqs. (29) and (30)]).

The TD voltage responses of the TL have been calculated for the power-exponential pulse (37) with $i_{\mathrm{m}} = 1.0$ A, $n = 2$ and $c_0 t_{\mathrm{w}} = 2\ell$ above both ideal PEC ground and a lossy half-space. Fig. 7 shows the far-end voltage responses above the PEC ground and lossy half-space with electric conductivity $\sigma = 4.0$ S/m and relative permittivity $\epsilon_r = 81$ (= sea water). For further validation, the TD response above the PEC ground has also been computed using the finite-integration technique (FIT) as implemented in CST Studio Suite. Despite fundamental differences in the models, the results, practically, coincide. It has also been verified that the voltage corrections for good conductors (e.g., copper, aluminum, and steel) can be for the present configuration virtually neglected.

1) The presented TD model can be extended to multiconductor TLs. A rigorous methodology to incorporate the mutual EM coupling between conductors is presented in [33] and [34, Sec. 15.4].
2) Finally, in this article, we have evaluated the open-circuit voltage as observed at one TL terminal, while the second one is loaded by the characteristic impedance. A straightforward approach to incorporate arbitrary loads is described in [35].

VII. Conclusion

The interaction of pulsed nonuniform EM fields with a uniform TL has been studied analytically with the aid of the TD Lorentz reciprocity theorem. It has been shown that a dedicated CdH-like inversion technique provides straightforward closed-form expressions for the pulsed EM fields radiated from the horizontal conductor of a TL, thus enabling the efficient evaluation of the EM coupling directly in TD. The proposed solution methodology is illustrated on the calculation of transient voltages induced by an impulsive VED source, for which a closed-form analytical solution is available. The use of such a referential solution has decisively confirmed the

validity of the new reciprocity-based coupling model. Finally, extensions of the TD model have been discussed.

APPENDIX A
INVERSE TRANSFORM OF GENERIC CONSTITUENTS

Following the methodology presented in [23], we shall carry out the inverse transform of generic integral expressions pertaining to the EM radiation by right- and left-going current pulses on the TL.

A. Right-Going Traveling-Wave Constituent

Upon substituting the s-domain counterpart of (7) in (17), it is found that a generic radiated EM-wavefield constituent can be expressed in the following way

$$\hat{\Gamma}_+(\boldsymbol{r},s)=\int_{x_+=x_1}^{x_2}\frac{\exp\{-s[R_+ +(x_+ -x_1)]/c_0\}}{4\pi R_+}\mathrm{d}x_+ \tag{38}$$

where we used $R_+=[(x-x_+)^2+d^2]^{1/2}$ with $d^2=(y-y_0)^2+(z-z_0)^2$. To cast (38) into the form that resembles the Laplace-transform integral [see (1)], we use

$$\frac{x_+ -x_1}{c_0}+\frac{R_+}{c_0}=\tau,\quad \text{for } \{\tau\in\mathbb{R};\tau>0\}. \tag{39}$$

Solving (39) for x_+, it is found that

$$x_+(\tau)=\frac{c_0\tau+x-x_1}{2}-\frac{1}{2}\frac{d^2}{c_0\tau-(x-x_1)}+x_1 \quad \text{for } \left\{T_1^+\le\tau\le T_2^+\right\} \tag{40}$$

where

$$T_1^+=\left[(x-x_1)^2+d^2\right]^{1/2}/c_0, \tag{41}$$

$$T_2^+=\ell/c_0+\left[(x-x_2)^2+d^2\right]^{1/2}/c_0. \tag{42}$$

Consequently, using (39) and (40) we get

$$R_+(\tau)=\frac{1}{2}\frac{[c_0\tau-(x-x_1)]^2+d^2}{c_0\tau-(x-x_1)}. \tag{43}$$

The Jacobian of the mapping can be then expressed in the following way

$$\partial_\tau x_+=R_+(\tau)/\Delta_+(\tau),\quad \text{for } \left\{T_1^+\le\tau\le T_2^+\right\} \tag{44}$$

where

$$\Delta_+(\tau)=\tau-(x-x_1)/c_0. \tag{45}$$

Hence, using (39) with (41)–(45), we end up with

$$\hat{\Gamma}_+(\boldsymbol{r},s)=\int_{\tau=T_1^+}^{T_2^+}\exp(-s\tau)\frac{\mathrm{d}\tau}{4\pi\Delta_+(\tau)}. \tag{46}$$

Finally, relying on Lerch's uniqueness theorem [29, Appendix], it can be concluded upon inspection that the desired TD original follows as described

$$\Gamma_+(\boldsymbol{r},t)=\frac{\mathrm{H}(t-T_1^+)-\mathrm{H}(t-T_2^+)}{4\pi\Delta_+(t)}. \tag{47}$$

The corresponding image-source wave constituent, say $\Gamma_+^*(\boldsymbol{r},t)$, is easily obtained from (47) by replacing $d^2=(y-y_0)^2+(z-z_0)^2$ with $d^{*2}=(y-y_0)^2+(z+z_0)^2$. In the same manner, we may find $x_+^*(\tau)$ and $R_+^*(\tau)$ from (40) and (43), respectively.

B. Left-Going Traveling-Wave Constituent

Upon substituting the s-domain counterpart of (10) in (17), it is found that a generic radiated EM-wavefield constituent can be expressed as below

$$\hat{\Gamma}_-(\boldsymbol{r},s)=\int_{x_-=x_1}^{x_2}\frac{\exp\{-s[R_- +(x_2-x_-)]/c_0\}}{4\pi R_-}\mathrm{d}x_- \tag{48}$$

where we used $R_-=[(x-x_-)^2+d^2]^{1/2}$ with $d^2=(y-y_0)^2+(z-z_0)^2$. To cast (48) into the Laplace-transform integral we may use the following mapping [see (39)]:

$$\frac{x_2-x_-}{c_0}+\frac{R_-}{c_0}=\tau,\quad \text{for } \{\tau\in\mathbb{R};\tau>0\}. \tag{49}$$

Solving (49) for x_- we find that [see (40)]

$$x_-(\tau)=-\frac{c_0\tau+x_2-x}{2}+\frac{1}{2}\frac{d^2}{c_0\tau-(x_2-x)}+x_2 \quad \text{for } \left\{T_1^-\le\tau\le T_2^-\right\} \tag{50}$$

where

$$T_1^-=\left[(x-x_2)^2+d^2\right]^{1/2}/c_0, \tag{51}$$

$$T_2^-=\ell/c_0+\left[(x-x_1)^2+d^2\right]^{1/2}/c_0. \tag{52}$$

Consequently, via (49) and (50) we get

$$R_-(\tau)=\frac{1}{2}\frac{[c_0\tau-(x_2-x)]^2+d^2}{c_0\tau-(x_2-x)}. \tag{53}$$

The Jacobian of the mapping can be then expressed in the following way.

$$\partial_\tau x_-=-R_-(\tau)/\Delta_-(\tau),\quad \text{for } \left\{T_1^-\le\tau\le T_2^-\right\} \tag{54}$$

where

$$\Delta_-(\tau)=\tau-(x_2-x)/c_0. \tag{55}$$

Finally, using (49) with (51)–(55), we arrive at

$$\hat{\Gamma}_-(\boldsymbol{r},s)=\int_{\tau=T_1^-}^{T_2^-}\exp(-s\tau)\frac{\mathrm{d}\tau}{4\pi\Delta_-(\tau)} \tag{56}$$

which yields, by virtue of Lerch's uniqueness theorem [29, Appendix], the TD counterpart of (48), i.e.,

$$\Gamma_-(\boldsymbol{r},t)=\frac{\mathrm{H}(t-T_1^-)-\mathrm{H}(t-T_2^-)}{4\pi\Delta_-(t)}. \tag{57}$$

The corresponding image-source wave constituent, say $\Gamma_-^*(\boldsymbol{r},t)$, is easily obtained from (57) by replacing $d^2=(y-y_0)^2+(z-z_0)^2$ with $d^{*2}=(y-y_0)^2+(z+z_0)^2$. In the same manner, we may find $x_-^*(\tau)$ and $R_-^*(\tau)$ from (50) and (53), respectively.

APPENDIX B
REFERENCE TD SOLUTION

The VED-induced voltages on a TL have been expressed analytically in closed form in [13] (see also [15, Ch. 13]) using the CdH technique [21]. For the convenience of the reader, these referential results are next briefly summarized.

To begin with, the open-circuit Thévenin voltage, as induced at $x = x_1$, can be expressed in the following way

$$V_1^{\mathrm{G}}(t) = -\mathcal{Q}(x_1|x_2, y_0, z_S - z_0, t) + \mathcal{Q}(x_1|x_2, y_0, z_0 + z_S, t) + \mathcal{V}(x_1, y_0, t) - \mathcal{V}(x_2, y_0, t - \ell/c_0) \quad \text{for } \{0 < z_0 < z_S\} \tag{58}$$

and

$$V_1^{\mathrm{G}}(t) = \mathcal{Q}(x_1|x_2, y_0, z_0 - z_S, t) + \mathcal{Q}(x_1|x_2, y_0, z_0 + z_S, t) + \mathcal{V}(x_1, y_0, t) - \mathcal{V}(x_2, y_0, t - \ell/c_0) \quad \text{for } z_0 > z_S \tag{59}$$

where

$$\mathcal{Q}(x_1|x_2, y, z, t) = \zeta_0 \ell^{\mathrm{R}}\, \partial_t i^{\mathrm{R}}(t) *_t \big[\mathcal{I}(x_2, y, z, t - \ell/c_0) - \mathcal{I}(x_1, y, z, t)\big]. \tag{60}$$

In (60) we have used

$$\mathcal{I}(x, y, z, t) = \frac{z}{4\pi(y^2 + z^2)} \mathcal{P}(x, y, z, t) \mathrm{H}(t - R/c_0) \tag{61}$$

with

$$\mathcal{P}(x, y, z, t) = \frac{1}{Rc_0 t}\left[xc_0 t - x^2 - \frac{R\big(c_0^2 t^2 - x^2\big) + c_0 t\big(y^2 + z^2\big)}{R + c_0 t} + \frac{c_0^2 t^2 \big(y^2 + z^2\big)}{R^2}\right]. \tag{62}$$

In (58) and (59), we have further used

$$\mathcal{V}(x, y, t) = \mathcal{U}(x, y, z_S - z_0, t) - \mathcal{U}(x, y, z_0 + z_S, t) \quad \text{for } \{0 < z_0 < z_S\} \tag{63}$$

and

$$\mathcal{V}(x, y, t) = 2\mathcal{U}(x, y, 0, t) - \mathcal{U}(x, y, z_0 - z_S, t) - \mathcal{U}(x, y, z_0 + z_S, t), \quad \text{for } z_0 > z_S \tag{64}$$

with

$$\mathcal{U}(x, y, z, t) = \zeta_0 \ell^{\mathrm{R}}\, \partial_t i^{\mathrm{R}}(t) *_t \mathcal{J}(x, y, z, t) \tag{65}$$

where

$$\mathcal{J}(x, y, z, t) = \left[\frac{1}{\big(c_0^2 t^2 - x^2 - y^2\big)^{1/2}} - \frac{zc_0 t}{R^3}\right] \frac{\mathrm{H}(t - R/c_0)}{4\pi}. \tag{66}$$

The TD voltage response at $x = x_2$ can be expressed in a similar fashion.

$$V_2^{\mathrm{G}}(t) = -\mathcal{Q}(-x_2| - x_1, y_0, z_S - z_0, t) + \mathcal{Q}(-x_2| - x_1, y_0, z_0 + z_S, t) + \mathcal{V}(x_2, y_0, t) - \mathcal{V}(x_1, y_0, t - \ell/c_0) \quad \text{for } \{0 < z_0 < z_S\} \tag{67}$$

and

$$V_2^{\mathrm{G}}(t) = \mathcal{Q}(-x_2| - x_1, y_0, z_0 - z_S, t) + \mathcal{Q}(-x_2| - x_1, y_0, z_0 + z_S, t) + \mathcal{V}(x_2, y_0, t) - \mathcal{V}(x_1, y_0, t - \ell/c_0) \quad \text{for } z_0 > z_S. \tag{68}$$

These TD expressions have been implemented in MATLAB and used in Section V to validate the reciprocity-based coupling model.

REFERENCES

[1] G. Tzeremes, P. Kirawanich, C. Christodoulou, and N. Islam, "Transmission lines as radiating antenna in sources aperture interactions in electromagnetic topology simulations," *IEEE Antennas Wireless Propag. Lett.*, vol. 3, pp. 283–286, 2004.

[2] J. Guo, Y.-Z. Xie, F. Rachidi, K.-J. Li, and S.-F. Wang, "On nonuniform transient electromagnetic field coupling to overhead transmission lines," *IEEE Trans. Antennas Propag.*, vol. 66, no. 6, pp. 3087–3096, Jun. 2018.

[3] K.-J. Li, Y.-Z. Xie, F. Zhang, and Y.-H. Chen, "Statistical inference of serial communication errors caused by repetitive electromagnetic disturbances," *IEEE Trans. Electromagn. Compat.*, vol. 62, no. 4, pp. 1160–1168, Aug. 2020.

[4] H. Tirmizi, D. Vanoost, J. Lannoo, G. A. E. Vandenbosch, and D. Pissoort, "Symbol diversity as a means to make PAM-4 modulation more resilient in harsh electromagnetic environments," *IEEE Trans. Electromagn. Compat.*, vol. 64, no. 6, pp. 1949–1957, Dec. 2022.

[5] C. Taylor, R. Satterwhite, and C. Harrison, "The response of a terminated two-wire transmission line excited by a nonuniform electromagnetic field," *IEEE Trans. Antennas Propag.*, vol. AP-13, no. 6, pp. 987–989, Nov. 1965.

[6] A. Agrawal, H. Price, and S. Gurbaxani, "Transient response of multiconductor transmission lines excited by a nonuniform electromagnetic field," *IEEE Trans. Electromagn. Compat.*, vol. EMC-22, no. 2, pp. 119–129, May 1980.

[7] V. Cooray and N. Theethayi, "Pulse propagation along transmission lines in the presence of corona and their implication to lightning return strokes," *IEEE Trans. Antennas Propag.*, vol. 56, no. 7, pp. 1948–1959, Jul. 2008.

[8] F. Rachidi, "A review of field-to-transmission line coupling models with special emphasis to lightning-induced voltages on overhead lines," *IEEE Trans. Electromagn. Compat.*, vol. 54, no. 4, pp. 898–911, Aug. 2012.

[9] P. Xiao et al., "Eigenmode-BLT-based method for calculating the coupling to microstrip antenna inside a cavity," *IEEE Trans. Antennas Propag.*, vol. 70, no. 5, pp. 3515–3522, May 2022.

[10] M. Štumpf and G. Antonini, "Electromagnetic field coupling to a transmission line—A reciprocity-based approach," *IEEE Trans. Electromagn. Compat.*, vol. 62, no. 2, pp. 461–469, Apr. 2020.

[11] A. T. de Hoop, *Handbook of Radiation and Scattering of Waves*. London, U.K.: Academic, 1995.

[12] M. Štumpf and G. Antonini, "Lightning-induced voltages on transmission lines over a lossy ground—An analytical coupling model based on the Cooray–Rubinstein formula," *IEEE Trans. Electromagn. Compat.*, vol. 62, no. 1, pp. 155–162, Feb. 2020.

[13] M. Štumpf, "Pulsed vertical-electric-dipole excited voltages on transmission lines over a perfect ground—A closed-form analytical description," *IEEE Antennas Wireless Propag. Lett.*, vol. 17, pp. 1656–1658, 2018.

[14] M. Štumpf, G. Antonini, and I. E. Lager, "Pulsed EM field transfer between a horizontal electric dipole and a transmission line—A closed-form model based on the Cagniard–de hoop technique," *IEEE Trans. Antennas Propag.*, vol. 68, no. 4, pp. 2911–2918, Apr. 2020.

[15] M. Štumpf, *Time-Domain Electromagnetic Reciprocity in Antenna Modeling*. Hoboken, NJ, USA: IEEE Press, 2019.

[16] J. L. Lagos and F. Fiori, "Worst-case induced disturbances in digital and analog interchip interconnects by an external electromagnetic plane wave—Part I: Modeling and algorithm," *IEEE Trans. Electromagn. Compat.*, vol. 53, no. 1, pp. 178–184, Feb. 2011.

[17] F. Vanhee, D. Pissoort, J. Catrysse, G. A. E. Vandenbosch, and G. G. E. Gielen, "Efficient reciprocity-based algorithm to predict worst case induced disturbances on multiconductor transmission lines due to incoming plane waves," *IEEE Trans. Electromagn. Compat.*, vol. 55, no. 1, pp. 208–216, Feb. 2013.

[18] T. Liang and Y.-Z. Xie, "Determining incidence and polarization of electromagnetic field for maximal/minimal coupling to transmission line system," *IEEE Microw. Wireless Compon. Lett.*, vol. 30, no. 11, pp. 1021–1024, Nov. 2020.

[19] M. Mehri and A. Amini, "Stochastic EMI noise model of PCB layout for circuit-level analysis of system in IoT applications," *IEEE Trans. Microw. Theory Techn.*, vol. 68, no. 12, pp. 5072–5081, Dec. 2020.

[20] A. T. de Hoop, I. E. Lager, and V. Tomassetti, "The pulsed-field multiport antenna system reciprocity relation and its applications—A time-domain approach," *IEEE Trans. Antennas Propag.*, vol. 57, no. 3, pp. 594–605, Mar. 2009.

[21] A. T. de Hoop, "A modification of Cagniard's method for solving seismic pulse problems," *Appl. Sci. Res.*, vol. 8, no. 1, pp. 349–356, 1960.
[22] L. B. Felsen and F. Capolino, "Time-domain Green's function for an infinite sequentially excited periodic line array of dipoles," *IEEE Trans. Antennas Propag.*, vol. 48, no. 6, pp. 921–931, Jun. 2000.
[23] D. Quak, "Analysis of transient radiation of a (traveling) current pulse on a straight wire segment," in *Proc. IEEE EMC Int. Symp. Symp. Record. Int. Symp. Electromagn. Compat.*, vol. 2, Montreal, QC, Canada, Jul. 2001, pp. 849–854.
[24] E. J. Rothwell, M. J. Cloud, and P. Ilavarasan, "Transient field produced by a traveling-wave wire antenna," *IEEE Trans. Electromagn. Compat.*, vol. 33, no. 3, pp. 172–178, Aug. 1991.
[25] G. S. Smith, "Teaching antenna radiation from a time-domain perspective," *Amer. J. Phys.*, vol. 69, no. 3, pp. 288–300, Mar. 2001.
[26] A. Sutinjo, M. Okoniewski, and R. Johnston, "Radiation from fast and slow traveling waves," *IEEE Antennas Propag. Mag.*, vol. 50, no. 4, pp. 175–181, Aug. 2008.
[27] M. Štumpf, J. Gu, and I. E. Lager, "Time-domain electromagnetic leaky waves," *IEEE Trans. Antennas Propag.*, vol. 71, no. 4, pp. 3382–3392, Apr. 2023.
[28] J. Gu, M. Štumpf, A. Neto, and I. E. Lager, "Pulsed operation of a weakly-dispersive, leaky-wave antenna: A causal numerical study," *IEEE Trans. Antennas Propag.*, vol. 72, no. 1, pp. 720–732, Dec. 2024.
[29] M. Štumpf, *Electromagnetic Reciprocity in Antenna Theory*. Hoboken, NJ, USA: IEEE Press, 2018.
[30] A. T. De Hoop, M. Stumpf, and I. E. Lager, "Pulsed electromagnetic field radiation from a wide slot antenna with a dielectric layer," *IEEE Trans. Antennas Propag.*, vol. 59, no. 8, pp. 2789–2798, Aug. 2011.
[31] V. Cooray, "Horizontal fields generated by return strokes," *Radio Sci.*, vol. 27, no. 4, pp. 529–537, Jul. 1992.
[32] M. Rubinstein, "An approximate formula for the calculation of the horizontal electric field from lightning at close, intermediate, and long range," *IEEE Trans. Electromagn. Compat.*, vol. 38, no. 3, pp. 531–535, Aug. 1996.
[33] M. Štumpf, I. E. Lager, and G. Antonini, "Time-domain analysis of thin-wire structures based on the cagniard-DeHoop method of moments," *IEEE Trans. Antennas Propag.*, vol. 70, no. 6, pp. 4655–4662, Jun. 2022.
[34] M. Štumpf, *Metasurface Electromagnetics: The Cagniard-DeHoop Time-Domain Approach*. London, U.K.: IET, 2022.
[35] M. Štumpf, G. Antonini, and J. Ekman, "Pulsed electromagnetic field coupling to a transmission line with arbitrary loads—A unified methodology based on reciprocity," *Electr. Power Syst. Res.*, vol. 227, Feb. 2024, Art. no. 109980.

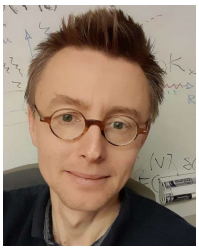

Martin Štumpf (Senior Member, IEEE) received the Ph.D. degree in electrical engineering from Brno University of Technology (BUT), Brno, Czech Republic, in 2011.

After his Ph.D. research, he spent a year and a half as a Post-Doctoral Fellow with KU Leuven, Leuven, Belgium. In 2018, he was a Visiting Professor at the UAq EMC Laboratory, University of L'Aquila, L'Aquila, Italy. He is currently an Associate Professor of theoretical electrical engineering with the Lerch Laboratory of EM Research, BUT, and a Visiting Researcher with the EISLAB, Luleå University of Technology, Luleå, Sweden. He has authored the books *Electromagnetic Reciprocity in Antenna Theory* (Wiley–IEEE Press, 2017), *Pulsed EM Field Computation in Planar Circuits: The Contour Integral Method* (CRC Press, 2018), *Time-Domain Electromagnetic Reciprocity in Antenna Modeling* (Wiley–IEEE Press, 2019), and *Metasurface Electromagnetics: The Cagniard-DeHoop Time-Domain Approach* (IET, 2022). His main research interests include modeling electromagnetic wave phenomena with an emphasis on antenna theory and EMC. Recently, he has been exploring analytical and numerical methods for computing the electromagnetic response of time-varying systems and devices.

Giulio Antonini (Fellow, IEEE) received the Laurea degree (cum laude) in electrical engineering from the University of L'Aquila, L'Aquila, Italy, in 1994, and the Ph.D. degree in electrical engineering from the University of Rome "La Sapienza," Rome, Italy, in 1998.

Since 1998, he has been with the UAq EMC Laboratory, University of L'Aquila, where he is currently a Professor. He has co-authored the book *Circuit Oriented Electromagnetic Modeling Using the PEEC Techniques* (Wiley–IEEE Press, 2017). His scientific research interests include computational electromagnetics.

Ioan E. Lager (Senior Member, IEEE) received the M.Sc. degree in electrical engineering from the "Transilvania" University of Braşov, Braşov, Romania, in 1987, the first Ph.D. degree in electrical engineering from Delft University of Technology, Delft, The Netherlands, 1996, and the second Ph.D. degree in electrical engineering from the "Transilvania" University of Braşov, in 1998.

He successively occupied several research and academic positions with the "Transilvania" University of Braşov and Delft University of Technology, where he is currently an Associate Professor. In 1997, he was a Visiting Scientist with Schlumberger-Doll Research, Ridgefield, CT, USA. He endeavors to bridge the gap between electromagnetic field theory and the design, implementation, and measurement of antenna front-end architectures. His research interests include applied electromagnetics, especially time-domain propagation and applications, and antenna engineering, with an emphasis on nonperiodic (interleaved) array antenna architectures.

Jonas Ekman (Member, IEEE) was born in Boden, Sweden, in 1972. He received the Ph.D. degree in electrical engineering from the Luleå University of Technology (LTU), Luleå, Sweden, in 2003.

From 2003 to 2007, he was a Researcher with LTU. From 2005 to 2006, he was a Post-Doctoral Researcher in full-wave, time domain, and PEEC modeling at the EMC Laboratory, University of L'Aquila, L'Aquila, Italy. In 2014, he was appointed as a Full Professor. Since 2022, he has been chairing the group of Electronic Systems with LTU. His research interests include computational electromagnetics, in particular, the use of the PEEC method for realistic electromagnetic modeling.